THE JOURNAL OF BIOLOGICAL CHEMISTRY VOL. 290, NO. 32, pp. 19853–19862, August 7, 2015

Bacteria May Cope Differently from Similar Membrane Damage Caused by the Australian Tree Frog Antimicrobial Peptide Maculatin 1.1*

Received for publication, February 3, 2015, and in revised form, May 26, 2015 Published, JBC Papers in Press, June 22, 2015, DOI 10.1074/jbc.M115.643262

Marc-Antoine Sani[‡1], **Sónia Troeira Henriques**[§2], **Daniel Weber**[‡], **and Frances Separovic**[‡]

From the [‡]*School of Chemistry, Bio21 Institute, The University of Melbourne, Parkville, Victoria 3010, Australia and the* [§]*Institute for Molecular Bioscience, University of Queensland, St. Lucia, Queensland 4072, Australia*

Background: Mac1 specificity and bactericidal concentrations may be due to a distinctive membrane disrupting mechanism.
Results: *S. aureus* growth is inhibited at 16-fold lower Mac1 concentration than *E. coli*, but both lipid membranes are compromised at similar concentrations.
Conclusion: Bacteria may cope differently with membrane damage.
Significance: Antimicrobial peptide mode of action needs to be better understood to develop new drug candidate.

Maculatin 1.1 (Mac1) is an antimicrobial peptide from the skin of Australian tree frogs and is known to possess selectivity toward Gram-positive bacteria. Although Mac1 has membrane disrupting activity, it is not known how Mac1 selectively targets Gram-positive over Gram-negative bacteria. The interaction of Mac1 with *Escherichia coli*, *Staphylococcus aureus*, and human red blood cells (hRBC) and with their mimetic model membranes is here reported. The peptide showed a 16-fold greater growth inhibition activity against *S. aureus* (4 μM) than against *E. coli* (64 μM) and an intermediate cytotoxicity against hRBC (30 μM). Surprisingly, Sytox Green uptake monitored by flow cytometry showed that Mac1 compromised both bacterial membranes with similar efficiency at ~20-fold lower concentration than the reported minimum inhibition concentration against *S. aureus.* Mac1 also reduced the negative potential of *S. aureus* and *E. coli* membrane with similar efficacy. Furthermore, liposomes mimicking the cell membrane of *S. aureus* (POPG/TOCL) and *E. coli* (POPE/POPG) were lysed at similar concentrations, whereas hRBC-like vesicles (POPC/SM/Chol) remained mostly intact in the presence of Mac1. Remarkably, when POPG/TOCL and POPE/POPG liposomes were co-incubated, Mac1 did not induce leakage from POPE/POPG liposomes, suggesting a preference toward POPG/TOCL membranes that was supported by surface plasma resonance assays. Interestingly, circular dichroism spectroscopy showed a similar helical conformation in the presence of the anionic liposomes but not the hRBC mimics. Overall, the study showed that Mac1 disrupts bacterial membranes in a similar fashion before cell death events and would preferentially target *S. aureus* over *E. coli* or hRBC membranes.

Antimicrobial peptides (AMPs)[3] are found in virtually all organisms including plants, insects, bacteria, and mammals as part of their innate immune system and act as endogenous antibiotics (1). The first AMPs were discovered more than 75 years ago but have not emerged as commercially viable drug candidates in contrast to naturally occurring small molecule compounds such as penicillin and, more recently, carbapenem. Because pathogenic bacteria are dangerously gaining the capability to render almost all antibiotics inefficient by slightly modifying the structure of targets (often cell receptors or enzymes) or by reducing the permeability of their lipid membranes (2), AMPs have regained some interest as drug alternatives. Their key advantage compared with classic antibiotics comes from their proposed mode of action, whereby they compromise the lipid membranes instead of targeting an intracellular and stereo-specific structure (3). AMPs are usually positively charged and adopt amphipathic structures (*e.g.* α-helical conformation). These properties are essential for their capacity to insert into lipid membranes, as is their ability to target the anionic microbial membrane (4, 5). Indeed, there are major differences between microbial and mammalian cells, such as lipid membrane composition, transmembrane potential, and the presence/absence of a cell wall. Bacterial membranes possess high amounts of negatively charged phospholipids, such as cardiolipin (CL) and phosphatidylglycerol (PG) on the outer leaflet (6, 7). In contrast, the outer membrane of mammalian cells is mainly composed of neutral lipids: cholesterol (Chol), phosphatidylcholine (PC) phospholipids, and sphingomyelin (SM) (8). Therefore, cationic AMPs selectively target and disrupt anionic membranes of bacterial cells over neutral cell membranes from humans (9). Thus, establishing how AMPs distinguish between microbes and host cells and, in some cases, between

* This work was supported in part by Australian Research Council Grant DP140102127 (to F. S.). The authors declare that they have no conflicts of interest with the contents of this article.
[1] To whom correspondence should be addressed: School of Chemistry, University of Melbourne, Parkville, 3010 VIC, Australia. Tel.: 61-3834-42436; Fax: 61-3934-78189; E-mail: msani@unimelb.edu.au.
[2] Recipient of Discovery Early Career Researcher Award DE120103152 from the Australian Research Council.

[3] The abbreviations used are: AMP, antimicrobial peptide; MIC, minimum inhibition concentration; RBC, red blood cell; hRBC, human RBC; MHB, Mueller Hinton broth; CL, cardiolipin; PG, phosphatidylglycerol; Chol, cholesterol; PC, phosphatidylcholine; SM, sphingomyelin; POPC, palmitoyloleoyl-phosphatidylcholine; POPG, palmitoyloleoyl-phosphatidylglycerol; TOCL, tetraoeloyl-cardiolipin; CF, 5(6)-carboxyfluorescein; MHB, Mueller Hinton broth; LUV, large unilamellar vesicles.

Gram-positive and Gram-positive bacteria, is of importance. Furthermore, the link between compromising the bacterial cell membrane and the AMP bactericidal effect is often not clear. This is partially due to the difficulty in matching *in vivo* and *in vitro* conditions with molecular level details.

In this study, we used maculatin 1.1 (Mac1), an AMP expressed in the skin of the Australian tree frog *Litoria genimaculata* (10), to investigate the link between the membrane activity of the peptide and the death of bacteria or red blood cells. Mac1 is a relatively short (21 amino acids) and weakly cationic (+1 net charge) peptide. It has been reported that Mac1 has weak bactericidal activities against Gram-negative bacteria and human red blood cells (hRBC) but is highly potent against Gram-positive bacteria (11). Furthermore, the D-amino acid enantiomer of Mac1 was shown to have similar activity to the L-enantiomer, indicating a mode of action independent of a membrane receptor (12). Previous studies have shown that Mac1 adopts an α-helical secondary structure in contact with lipid membranes (13). The helical peptide is amphipathic and can insert into lipid bilayers, eventually forming pores (14).

To gain molecular detail on the interaction of Mac1 with the lipid bilayer in cell membranes, bioassays with hRBC, *Escherichia coli*, or *Staphylococcus aureus* were compared with biophysical assays performed using membrane models that mimicked their respective lipid compositions. The *E. coli* membrane model consisted of POPE/POPG (7:3) (7), *S. aureus* of POPG/TOCL (3:2) (6), and red blood cells of POPC/SM/Chol (1:1:1) (8). Flow cytometry and dye leakage assays were used to determine the concentration of Mac1 necessary to compromise membrane integrity, whereas ζ-potential assays monitored the perturbation on the membrane potentials. The peptide affinity for a particular lipid membrane composition was followed by surface plasmon resonance and a novel competitive dye leakage assay (15). The results were compared with the bactericidal and hemolytic concentrations to discuss the mechanism by which Mac1 kills bacteria and hRBC.

Experimental Procedures

Materials—Maculatin 1.1 (GLFGVLAKVAAHVVPAIAEHF-NH_2; molecular weight, 2148) at >95% purity was purchased from Federation Bioscience (Melbourne, Australia). Melittin (GIGAVLKVTTGLPALISWIKRKRQQ-NH_2; molecular weight, 2846.5) was purchased from Mimotopes (Melbourne, Australia). The peptide was washed in 5 mM HCl and lyophilized overnight to remove residual trifluoroacetic acid (16). Palmitoyloleoyl-phosphatidylcholine (POPC), palmitoyloleoyl-phosphatidylglycerol (POPG), tetraoeloyl-cardiolipin (TOCL), and sphingomyelin (SM) phospholipids were purchased from Avanti Polar Lipids (Alabaster, AL) and used without further purification. LPS purified from *E. coli* O127:B8 (L3129; Sigma), cholesterol, 5(6)-carboxyfluorescein (CF), and Triton X-100 were purchased from Sigma. PD-10 columns were purchased from GE Healthcare (VWR, Brisbane, Australia).

Hemolytic Assay—Hemolysis induced by Mac1 was determined against hRBC and monitored by hemoglobin release. Briefly, hRBCs were isolated from fresh blood by centrifugation at 4000 rpm (1500 × *g*) for 1 min, washed, and diluted in PBS (137 mM NaCl, 2.7 mM KCl, 10 mM Na_2HPO_4, 1.8 mM KH_2PO_4, pH 7.4) to a final concentration of 0.25% (v/v). The peptide was incubated with hRBC in a round-bottomed 96-well plate for 1 h at 37 °C, assayed in triplicate with 2-fold dilutions of peptide starting from 64 μM. After incubation, nonlysed cells were pelleted by centrifugation at 1500 rpm (~500 g), the supernatant was transferred to a flat-bottom plate, and released hemoglobin from lysed cells was quantified by absorbance at 405 nm (A_{sample}). Melittin, a membrane-permeable and hemolytic peptide, was used as a positive control. Triton X-100 (0.1% (v/v)) and PBS were included to establish 100% (A_{Triton}) and 0% of lysis (A_{PBS}), respectively. The percentage of hemolysis was calculated using the following equation.

$$\%\ \text{haemolysis} = (A_{sample} - A_{PBS})/(A_{Triton} - A_{PBS}) \times 100 \quad \text{(Eq. 1)}$$

Antimicrobial Susceptibility—Susceptibility of bacteria to Mac1 was considered in terms of bacterial growth inhibition concentrations. A microtitre broth dilution method was employed (17). Gram-negative *E. coli* ATCC 25922 (type strain, smooth LPS), *E. coli* CGSC 5167 (strain with rough LPS), and Gram-positive *S. aureus* ATCC 25923 were tested. Briefly, bacterial suspensions grown in Mueller Hinton broth (MHB) to exponential phase ($A_{600} = 0.5$) were diluted to 5×10^5 cells/ml in MHB and incubated with 2-fold dilutions of peptides (solubilized in sterile water) in 96-well nonbinding surface plates (Corning) for 24 h at 37 °C. The minimal inhibitory concentration (MIC) was the lowest concentration showing no visible growth. The ability to inhibit growth was further confirmed by adding 30 μl of resazurin dye (0.01% (w/v)) to each well. The plates were incubated at 37 °C for further 18 h. Wells with pink coloration indicate reduction of resazurin and, therefore, bacterial growth, whereas blue coloration indicates death of organisms or not enough organisms to reduce resazurin (18). The MIC value is the lowest peptide concentration of the wells with blue coloration. The assays were done in triplicate.

Cytotoxicity Studies against Cultured Cells—Cervical cancer (HeLa) and breast cancer (mcf-7) cells were grown in T175 flasks with DMEM (supplemented with 10% (v/v) of fetal bovine serum and 1% (w/v) penicillin/streptomycin) and incubated in humidified atmosphere at 37 °C with 5% CO_2. The day before the assay, cells were seeded (5×10^3 cells/well) in 96-well flat-bottomed plates. Mac1 and melittin were incubated for 2 h in concentrations ranging from 40 to 0.35 μM (final volume, 100 μl) in media without serum to avoid degradation. Controls without peptide or with Triton X-100 (0.01% (v/v) were included to establish 0 and 100% cell death, respectively. After 2 h of incubation, the peptide was removed, and the cells were washed with PBS. Fresh medium containing serum and resazurin dye (0.02% w/v) was added to the cells and incubated for 18 h. Absorbance was measured at 540 and 620 nm, and the percentage of cell death was determined as described elsewhere (18).

Microbial Membrane Permeabilization Detection by SYTOX Green Fluorescence Emission—*E. coli* ATCC 25922 and *S. aureus* ATCC 25923 cells with compromised membranes were detected with SYTOX® Green (Invitrogen), a DNA-bind-

ing dye that becomes fluorescent when bound to nucleic acids and only enters cells with a compromised plasma membrane (19). *E. coli* or *S. aureus* bacterial suspensions were grown in LB or MHB to exponential phase (A_{600} = 0.5). Cell suspensions were diluted to 10^7 cells/ml in MHB or in PBS. Bacterial suspensions in either PBS or MHB were incubated with Mac1 at different concentrations (4-fold dilutions from 64 μM) for 1 h at 37 °C with shaking. Sytox Green (2 μM) was incubated with peptide-treated cells for 10 min, and the fluorescence emission signal was evaluated by flow cytometry. The population of cells was selected based on forward scatter and side scatter measurements. Cells with compromised membranes were identified by fluorescence (excitation with 488-nm laser and detection at 530 nm with 30-nm bandpass). Mean fluorescence emission signal and percentage of fluorescent cells was determined by screening 50,000 cells. Each experiment was repeated at least three times. Flow cytometry measurements were performed with a BD FACSCanto II (BD Biosciences).

To examine whether cell permeability is inversely correlated with cell viability, peptide-treated and untreated samples with appropriate dilutions were spread in LB agar plates, and colony formation units were counted after 24 h incubation at 37 °C. The experiment was conducted six times.

CF Encapsulation in Large Unilamellar Vesicles—Large unilamellar vesicles encapsulating CF were prepared by suspending lipid films to 15 mM phospholipid in CF buffer (55 mM CF, 40 mM imidazole, 1 mM EDTA, adjusted to pH 7.4 with KOH and HCl). Solutions were freeze/thawed five times and then extruded 10 times through an Avanti Mini-Extruder using 0.1-μm polycarbonate filters to produce LUV of a nominal 100-nm diameter. Samples were extruded above the corresponding main gel to fluid chain melting temperatures of the phospholipids. Nonencapsulated dye was removed by gel filtration using a PD-10 desalting column with a 2.5-ml dead volume. 1 ml of each CF-loaded LUV lipid system was eluted under gravity with running buffer (40 mM imidazole, 110 mM KCl, 1 mM EDTA, pH 7.4). Approximately 2 ml was collected after passing 2.5 ml of running buffer. CF-free LUV were prepared similarly as CF-loaded LUV except that the lipid mixtures were suspended with 1 ml of the running buffer to reach a ~15 mM stock concentration. Phospholipid concentrations were determined in triplicate using a modified phosphorus assay as described previously (15).

CF Release Measurements in Single and Competitive Lipid Environments—Samples were prepared by mixing a 1:1 molar ratio of CF-loaded and CF-free vesicles and an appropriate amount of peptide stock solution to produce desired lipid to peptide molar ratios. Negative controls were made by substituting peptide stock for buffer-only and positive controls by adding Triton X-100 to a final 0.1% (v/v) concentration.

Measurements were made on a FLUOstar Optima plate reader (BMG Labtech) using a Falcon96 tissue culture 96-well plate (Fisher). The excitation wavelength was set at 492 nm, and the bottom-read emission was recorded at 520 nm. 10 reads (120 s cycle time) were performed at 30 °C with 5 s of orbital shaking prior to each cycle, and the fluorescence intensities were then averaged.

The percentage of CF fluorescence was obtained by normalizing the averaged intensities (I) against negative (baseline, I_{min}) and positive (100% release, I_{max}) controls, according to the following equation.

$$\%\text{fluorescence} = 100 \cdot (I - I_{min})/(I_{max} - I_{min}) \quad \text{(Eq. 2)}$$

The normalized intensities were plotted against the lipid to peptide molar ratio and fitted using an empirical logistic function,

$$F = F_{max} + (F_{max} - F_{min})/(1 + (x/x_0)^p) \quad \text{(Eq. 3)}$$

where F is the normalized intensity at each lipid to peptide ratio; F_{min} and F_{max} are fixed at 0 and 100%, respectively; x is the peptide concentration; x_0 is the peptide concentration necessary to obtain 50% of maximal fluorescence (LC_{50}); and p is a cooperativity factor (15).

Circular Dichroism Spectroscopy—Mac1 stock solutions of 1 mg/ml were prepared by dissolving lyophilized powder into CD buffer (20 mM phosphate, 1 mM NaCl, pH 7.4). The stock solution was sonicated (10 s) and vortexed prior to each use. LUV vesicles were prepared as described above for CF-free vesicles, except that lipid systems were resuspended into CD buffer. The lipid suspension was homogenized by extrusion to obtain LUVs with a diameter of 200 nm (10 times through polycarbonate membranes with 200-nm diameter pores). The size of the LUV was confirmed by dynamic light scattering. Peptide and LUV solutions were mixed to obtain samples with 160 μl of volume and 100 μM Mac1.

CD spectra were acquired on a Chirascan spectropolarimeter (Applied Photophysics Ltd, UK) between 180 and 260 nm using a 0.1-mm-path length cylindrical quartz cell (Starna, Hainault, UK). Spectra were acquired with 1-nm data intervals, 1-s integration time, and 2-scan accumulation. The signal was recorded as millidegrees at 25 °C. Spectra were zeroed at 260 nm and normalized to give units of mean residue ellipticity (MRE) according to $[\theta]_{MRE} = \theta/(c \times l \times N_r)$, where θ is the recorded ellipticity in millidegrees, c is the peptide concentration in dmol·liter^{-1}, l is the cell path length in cm, and N_r is the number of residues. The helical percentage (H_α) was calculated from the Luo-Baldwin formula [2],

$$H_\alpha\,(\%) = (\theta_{222\,nm} - \theta_c)/(\theta^{\infty}_{222\,nm} - \theta_C) \quad \text{(Eq. 4)}$$

where $\theta_C = 2200 - 53T$, $\theta^{\infty}_{222\,nm} = (-44{,}000 + 250\ T)(1 - k/N_{Residues})$, with T in °C and $k = 4$ as described for unrestricted peptides (20).

ζ-Potential Measurements—LUV were prepared as described in the CD section, except that 5 and 50 mM NaCl concentrations were used. Appropriate volumes of LUV (200 nm diameter) and Mac1 were mixed to produce individual samples at the desired lipid to peptide molar ratio and then transferred into a disposable cell (Malvern DTS 1060C) for ζ-potential measurements.

ζ-Potential measurements were performed using a Malvern Zetasizer Nano ZS apparatus (Malvern, UK) with backscattering detection at 173° and a constant voltage of 40 V. Measurements were performed in triplicate at 25 °C with 100 runs averaged per experiment. The viscosity and refractive index were

TABLE 1

Bactericidal, hemolytic, and anticancer activities and permeabilization to SYTOX Green induced by Mac1

All values are given in μM.

	E. coli ATCC 25922	*E. coli* CGSC 5167	*S. aureus* ATCC 25923
MIC[a]			
Mac1	64 (16–32)[b]	4–8	4 (16–64)[b]
Melittin	2 (32)[b]	0.02	0.5 (32)[b]
SYTOX Green uptake[c]			
Mac1	4.5 ± 0.5 (45.4 ± 2.9)[d]	2.1 ± 0.1	3.6 ± 0.3 (23.7 ± 3.0)[d]
Melittin	0.3 ± 0.1 (1.7 ± 0.1)[d]	0.11 ± 0.01	0.3 ± 0.1 (1.0 ± 0.1)[d]
Haemolytic and anticancer activity[e]	HeLa	MCF-7	hRBC
Mac1	>32	23.0 ± 0.30	29.5 ± 1.0
Melittin	1.1 ± 0.1	0.6 ± 0.1	1.2 ± 0.1

[a] MIC values were obtained with resazurin and tested in triplicate with 5×10^5 cells/ml in MHB medium.
[b] MIC values were obtained with resazurin and tested in triplicate with 5×10^5 cells/ml in LB medium.
[c] LC_{50} (concentration required to lyse 50% of the cells) was obtained in triplicate and followed by flow cytometry with 10^7 cells/ml. Mac1 was incubated with bacteria in PBS for 1 h at 37 °C, before the addition of SYTOX Green.
[d] Mac1 was incubated with bacteria in MHB for 1 h at 37 °C, washed, and resuspended in PBS before the addition of SYTOX Green.
[e] CC_{50} (concentration required to kill 50% of the cancer cells) was determined with 5×10^3 cells/well HeLa or MCF-7. HC_{50} (concentration required to induce lysis in 50% of the RBCs) was determined in triplicate with 0.25% (v/v) RBCs ($\sim 3 \times 10^4$ cells/ml). HC_{50}, CC_{50}, and LC_{50} and respective S.D. were obtained by fitting the data with a sigmoidal curve.

set at 0.8872 cP and 1.550, respectively. The monomodal analysis mode provided by the Malvern software was used to measure the ζ-potential upon Mac1 titration.

Peptide Membrane Binding Followed by Surface Plasmon Resonance—The affinity of Mac1 for model membranes composed of POPC/Chol/SM (1:1:1 molar ratio), POPE/POPG (7:3), and POPG/CL (3:2) was compared using surface plasmon resonance. A BIAcore 3000 system (Biacore, GE Healthcare) and a L1 Sensor Chip were used. Solutions were freshly prepared and filtered using a 0.22-μm-pore size filter. Small unilamellar vesicles (diameter, 50 nm) prepared by freeze-thaw fracturing and sized by extrusion were deposited onto the L1 Chip as previously described (21). Mac1 samples with different concentrations were injected over deposited lipid bilayers as described previously (22). All measurements were conducted at 25 °C; 10 mM HEPES buffer containing 150 mM NaCl, pH 7.4, was used as running buffer and to prepare vesicle suspensions and peptide samples. The lipid deposited onto the chip surface is dependent on the lipid mixture; therefore, for a more accurate comparison of the binding affinity for the different lipid mixtures, the response units were converted into peptide to lipid ratio (mol/mol) as described (23).

Results

Mac1 Has Antimicrobial Activity against S. aureus and E. coli and Low Hemolytic and Anticancer Activity—Mac1 displayed 10-fold greater potency for inhibiting growth of *S. aureus* than *E. coli* (Table 1), with MIC of 4 and 64 μM, respectively. These results are in agreement with previous reports suggesting that Mac1 is selective toward Gram-positive bacteria. Such preference was suggested to correlate with higher amount of negatively charged lipids in Gram-positive when compared with Gram-negative bacteria (24). Mac1 is less efficient in inhibiting the growth of bacteria than the bee venom peptide melittin, also known for its antimicrobial activity (25), with the latter inhibiting bacterial growth at 2 and 0.5 μM against *E. coli* and *S. aureus*, respectively (Table 1). Notably, a 4-fold greater potency against Gram-positive was also observed.

When incubated in growth medium with higher salt content (LB medium), MIC for both Mac1 and melittin were highly increased. Mac1 and melittin have been used in many experiments without showing any solubility or secondary structure perturbations in buffer with up to 150 mM NaCl (14, 15, 25). Therefore, it may be that bacteria are able to withstand harsh membrane damage in high salt (LB) compared with low salt growth medium (MHB).

An *E. coli* resistant strain with a rough LPS (no O-antigen chain) was used to investigate the effect of LPS at the outer membrane interface. Mac1 and melittin were both 10- and 100-fold more potent, respectively, at inhibiting the growth of the mutant compared with the *E. coli* type strain.

The effect of Mac1 on eukaryotic target hRBC was also evaluated using hemolytic assays. Although not hemolytic at concentrations that inhibit *S. aureus* growth, the concentration required to lyse 50% of hRBC (HC_{50}) is higher than the MIC against *E. coli* type strain (Table 1). However, the number of bacteria is greater than the number of RBC by ~17-fold, and therefore, at an equivalent hRBC concentration, Mac1 concentration would be extrapolated to be 17-fold greater. Considering the surface area of the RBC, ~120-fold greater than the area of a spherical *S. aureus* bacterium (~1.1 μm^2) and 40-fold for *E. coli* (~3.5 μm^2), the greater HC_{50} can also be explained by the greater amount of peptide necessary to cover the lipid membrane of RBCs *versus* bacteria. Although this would put the MIC against *S. aureus* within the same range, it does not correlate well with the MIC against *E. coli* strains. In contrast to the anionic microbial membrane surface, the outer leaflet of the hRBC membrane is mainly composed of zwitterionic lipids, producing a net neutral membrane. These observations suggest a preference toward negatively charged membranes over neutral membranes and that the lipid composition of the bacterial membranes plays a critical role in the antimicrobial activity of Mac1. Such interpretations are in agreement with previous studies (4, 13).

Finally, the activity of Mac1 was also tested against two cultured cancer lines: cervical (HeLa) and breast (mcf-7) cancer cells (Fig. 1). Cancer cells are known to have a more negative membrane surface compared with healthy cells, and therefore, cationic AMPs have been investigated as potential anticancer agents (26). The concentration of Mac1 required to kill 50% of

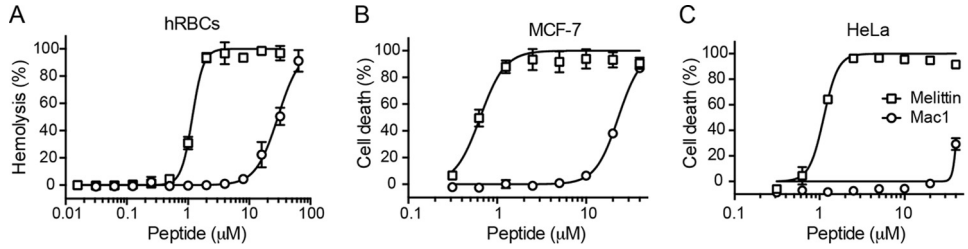

FIGURE 1. **Cytotoxicity of Mac1.** *A–C*, dose response against hRBC (*A*), HeLa cells (*B*), and MCF-7 cells (*C*). Human red blood cells (~3×10^4 cells/ml) and cancer cells (5×10^3 cells/well seeded in the day before) were incubated with various concentrations of peptide at 37 °C for 1 h (red blood cells) or 2 h (HeLa and mcf-7 cells). The percentage of hemolysis was determined by following release of hemoglobin into solution, and the percentage of dead HeLa or mcf-7 cells was determined by resazurin assay. The averages and S.D. of three replicates are shown.

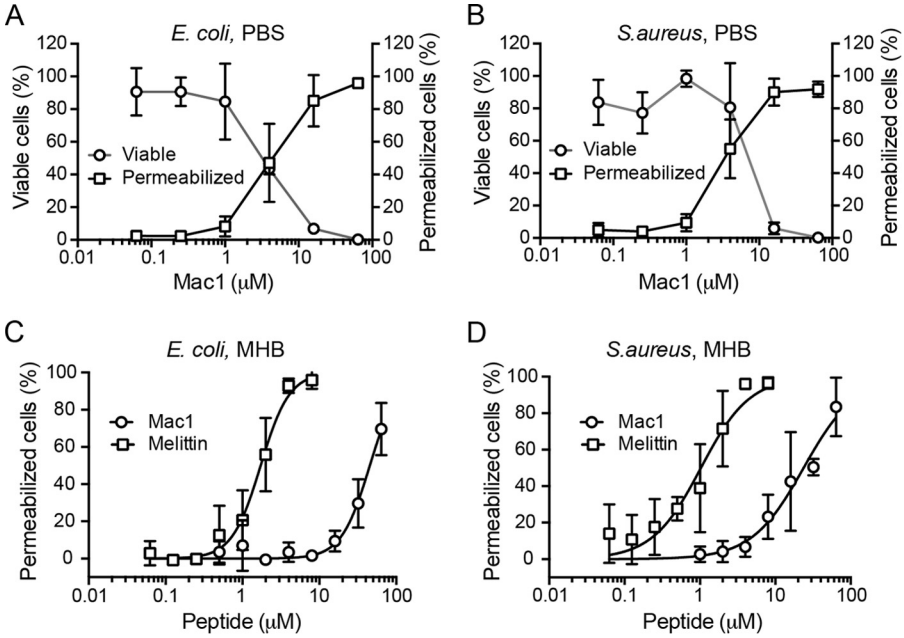

FIGURE 2. **Bacterial cell permeabilization in the presence of Mac1.** *A–D*, *E. coli* ATCC29522 (*A*) and *S. aureus* ATCC29523 (*B*) dispersed in PBS (10^7 cells/ml) or *E. coli* ATCC29522 (*C*) and *S. aureus* ATCC29523 (*D*) dispersed in MHB (10^7 cells/ml) were incubated with various concentrations of Mac1 or melittin at 37 °C for 1 h. Cell membrane permeabilization was detected by SYTOX Green fluorescence emission. The percentage of fluorescent cells was determined by flow cytometry. Viable cells were determined by colony formation unit counts in LB agar plates. The averages and S.D. of six (*A* and *B*) or three (*C* and *D*) replicates are shown.

the cells (CC_{50}) was >32 and 23 μM against HeLa and mcf-7 cells, respectively (Fig. 1 and Table 1). The dose-response curves and toxicity values were close to those found for hemolytic activity, suggesting a similar mode of action, probably dependent on membrane disruption. The activity against human cells suggests that electrostatic interactions alone are not sufficient to explain the lytic activity of Mac1 against cell membranes. Melittin, a peptide known to act through cell membrane disruption, had high toxicity against both cell lines, with CC_{50} values of 1.1 and 0.6 μM against HeLa and mcf-7, respectively.

Mac1 Permeates E. coli and S. aureus Membranes at Similar Concentrations—To further investigate the hypothesis that Mac1 kills the bacteria by membrane disruption, the membrane permeability to SYTOX Green dye was investigated using flow cytometry. SYTOX Green is nonfluorescent in aqueous environment but becomes fluorescent when interacting with nucleic acids and can only enter cells if membranes are compromised (19). Fig. 2 shows that 3 μM of Mac1 can permeate 50% of *S. aureus* bacteria (LC_{50}), and surprisingly, approximately the same concentration was required against *E. coli* type strain bacteria and just slightly lower against the rough LPS *E. coli* strain (2.1 μM). Such findings were not expected, considering the higher MIC obtained with *E. coli* type strain bacteria. Also, the population of viable bacteria incubated with Mac1 correlated with the percentage of nonpermeabilized membranes (Fig. 2).

To determine whether the growth medium had an effect, these experiments were repeated by incubating the peptide with bacterial suspensions in MHB, instead of PBS. The concentration of Mac1 necessary to induce permeabilization in 50% of the cells increased by 10-fold against *E. coli* and 7-fold against *S. aureus.* Similarly, an increase was observed with melittin: ~6-fold against *E. coli* and 4-fold against *S. aureus* (Table 1). Overall, the analogous increase in LC_{50} observed for both peptides against *S. aureus* and *E. coli* was consistent with the assay performed in PBS, and the greater concentrations are most likely due to the ongoing replication in nutrient-rich medium, whereas bacteria are not able to replicate in PBS. Strikingly, if the generation time (~15 min for *E. coli* and 30 min for *S. aureus*) is considered, the concentration of Mac1 necessary to lyse 10^7 cells/ml is approximately the same against both strains, 11 μM, and slightly greater than in PBS. Although

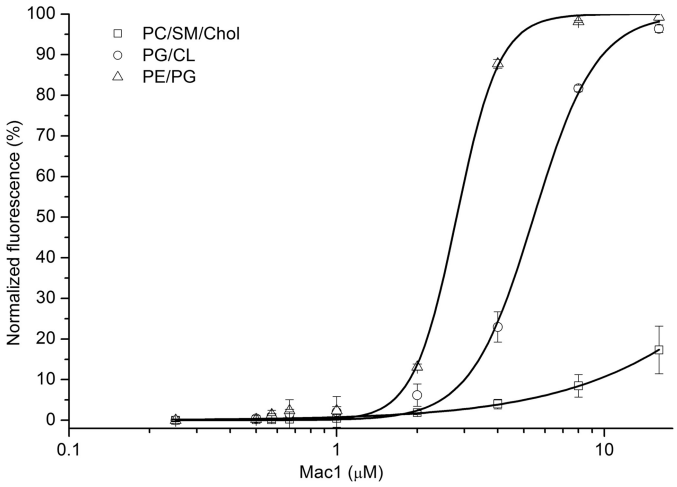

FIGURE 3. **CF leakage assays of POPC/SM/Chol (*squares*), POPE/POPG (*triangles*), and POPG/TOCL (*circles*) LUV incubated with Mac1.** Experiments were performed at 37 °C. Curve fitting was achieved using a logistic model.

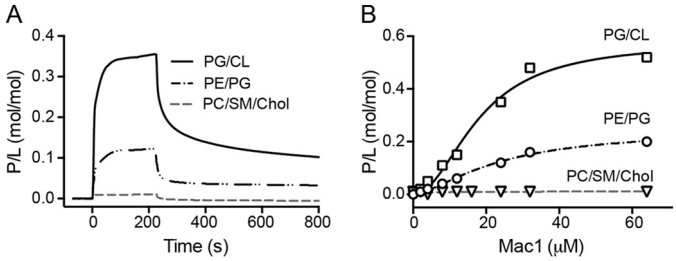

FIGURE 4. **Binding of Mac1 to lipid membranes studied by surface plasmon resonance.** *A*, sensorgrams obtained upon injection of 24 μM over POPC/Chol/SM (1:1:1 molar ratio), POPE/POPG (7:3 molar ratio), or POPG/TOCL (3:2 molar ratio) bilayers for 220 s (association phase). The dissociation from the membranes was followed after injection was stopped (dissociation phase). *B*, dose-response binding of Mac1 for POPC/Chol/SM (1:1:1), POPE/POPG (7:3), or POPG/TOCL (3:2) membranes. Peptide to lipid ratio (*P/L* mol/mol) at the end of association phase was determined to normalize the response to the total amount of lipid deposited onto chip surface (1 response units = 1 pg·mm^{-2} of peptide or lipid).

this estimation does not take into consideration the growth inhibition induced by Mac1, nor any active membrane damage repair, the concentration of Mac1 necessary to induce the uptake of SYTOX Green by *E. coli* and *S. aureus* remained well under the MIC.

Mac1 Induces Greater Leakage from Charged Vesicles—CF leakage assays were performed on vesicles mimicking the lipid compositions of the bacterial and hRBC membranes. This dye is similar in size to SYTOX Green used in the flow cytometry (6.5 Å radius). The membrane disruption upon AMP titration induces dequenching of the encapsulated dyes, and the increase in fluorescence is used to assess the effect of specific lipid composition on Mac1 lytic activity. The concentration of Mac1 required to induce leakage in 50% of the vesicles (final lipid concentration was 100 μM) made of POPE/POPG lipids, which mimic *E. coli* membranes, was 2-fold lower than from vesicles made of POPG/TOCL lipids, which mimic the membrane of *S. aureus* bacteria, with an LC_{50} of 2.8 ± 0.1 and 5.4 ± 0.2 μM, respectively. Interestingly, Mac1 has a low ability to induce leakage from POPC/SM/Chol vesicles (LC_{50} > 16 μM), here used to model the outer leaflet of hRBC membranes (Fig. 3). These results support the hypothesis that Mac1 has a greater lytic activity against bacterial membranes than against hRBC membranes but do not correlate with the MIC values obtained for *E. coli versus S. aureus* and the LC_{50} obtained with hRBC.

To examine whether the ability to induce vesicle leakage correlates with ability to bind membranes, the affinity of Mac1 for POPG/TOCL, POPE/POPG, and POPC/SM/Chol bilayers was compared by surface plasmon resonance. Mac1 has weak ability to bind POPC/SM/Chol membranes (Fig. 4) but has the ability to bind POPG/TOCL and POPE/POPG. A larger affinity for POPG/TOCL suggests that the overall charge of the membrane play a role in the Mac1 affinity for lipid bilayers and shows that Mac1 prefers membranes that mimic the properties of Gram-positive bacteria.

Mac1 Shows Greater Affinity for S. aureus versus E. coli Model Membranes in a Competitive Assay—The lytic activity of Mac1 was also investigated in conditions where vesicles with distinct lipid composition were mixed (*i.e.* Gram-negative model membranes mixed with Gram-positive model membranes or models of hRBC membranes mixed with either of the bacterial membrane models) using an approach previously developed to study the affinity of membrane-active peptide within a competitive lipid environment (15). As shown in Fig. 5, the concentration of Mac1 required to induce leakage in 50% of CF-loaded POPE/POPG vesicles in the presence of POPG/TOCL vesicles was 5-fold higher than in the situation with POPE/POPG vesicles only (Table 2). The peptide did not induce dye leakage from CF-loaded POPC/SM/Chol when in the presence of POPE/POPG or POPG/TOCL vesicles. The reverse experiments showed that the concentration of Mac1 required to induce 50% leakage from dye-filled POPG/TOCL *versus* POPE/POPG or POPC/SM/Chol vesicles decreased by 2-fold (Table 2). The same effect was observed for POPE/POPG vesicles mixed with POPC/SM/Chol vesicles. These results show that in conditions in which *S. aureus* and *E. coli* model membranes are mixed, Mac1 selects *S. aureus* model membranes, not obvious in assays in which these two model membranes are tested individually.

Membrane Depolarization Occurred at Similar Mac1 Concentrations—To evaluate whether Mac1 induces depolarization of the anionic bacterial membrane, the electric membrane potential of *E. coli* and *S. aureus* upon peptide titration was determined via ζ-potential measurements. The ζ-potential of *S. aureus* and *E. coli* bacteria was found to be −13 and −23 mV, respectively (Fig. 6). The titration of the cationic (+1) Mac1 peptide into the bacterial solutions induced a significant shift toward neutral ζ-potentials, inducing 55 and 35% decreases of ζ-potential for *S. aureus* and *E. coli*, respectively.

As expected, POPG/TOCL (100% anionic lipids) and POPE/POPG (30% anionic lipids) membranes also exhibited negative ζ-potentials (Fig. 6) but more negative than obtained for both bacteria, −50.5 and −39.5 mV, respectively, probably because of the presence of other charged components inserted into or adsorbed onto the bacterial membranes or the cell wall. The ζ-potential of POPG/TOCL and POPE/POPG vesicles upon Mac1 titration increased by 60 and 40%, respectively, in a similar trend as observed with *S. aureus* and *E. coli* ζ-potentials, although ionic concentration was slightly different.

Mac1 Has Higher Helical Content in Charged Lipid Systems—Determination of Mac1 secondary structure in the presence of bacteria and hRBC by CD spectroscopy is impaired because of a strong background signal from native proteins; therefore, CD spectroscopy measurements were conducted using PC/SM/Chol, PC/SM, PG/CL, PE/PG, LPS, CL, and PG vesicles. The CD spectrum obtained with Mac1 in buffer exhibited a band with negative minimum at ~190 nm, typical of random coil structures, suggesting that Mac1 is unstructured in aqueous environment, whereas in the presence of PE/PG or PG/CL vesicles, the CD spectra possess two minima at ~222 and 209 nm with a maximum at ~200 nm, indicating dominant α-helical secondary structures (Fig. 7*A*). Acquisition of an α-helical conformation when in a membrane environment is consistent with previous studies (13, 14). Interestingly, the CD spectrum of Mac1 in the presence of PC/SM/Chol was similar to the one obtained in buffer, indicating that the majority of the peptide molecules are in a random conformation, in agreement with Mac1 binding weakly to this particular membrane composition. Note that the PC/SM/Chol lipid-only background was strong, because of the presence of SM lipids, and the spectrum displayed in Fig. 7 was smoothed after subtracting the lipid-only background signal. The contribution of helical structure was slightly higher in the presence of PG/CL (~65%) than in the presence of PE/PG (~55%).

In the presence of LPS micelles, Mac1 also acquired α-helical confirmation (47%) (Fig. 7*A*), suggesting that LPS does not prevent peptide binding to *E. coli* membranes. Interestingly, higher α-helical content was obtained with POPG (65%) and TOCL (60%) compared with POPC (40%) and POPC/SM (45%) model membranes (Fig. 7*C*). These results indicate that Mac1 has a greater, but not specific, affinity for anionic lipids (POPG *versus* TOCL). Furthermore, the tight packing induced by the presence of Chol and SM inhibited Mac1 binding to the vesicles (see POPC/SM/Chol *versus* POPC/SM and POPC in Fig. 7*B*).

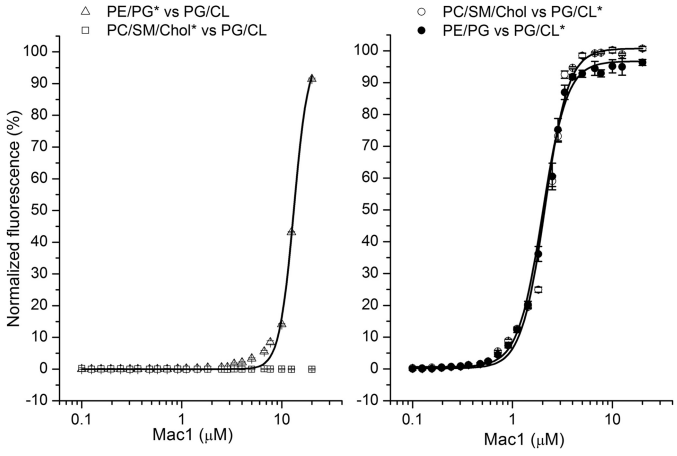

FIGURE 5. **CF leakage assay of Mac1 titration into a competitive lipid environments made of 50 μM of dye-filled LUV* and 50 μM of dye-free LUV.** *Left panel*, effect of the presence of POPG/TOCL LUV on Mac1 lytic activity against POPE/POPG* (*triangles*) and POPC/SM/Chol* (*squares*). *Right panel*, reverse experiments investigating Mac1 lytic activity against POPG/TOCL* LUV in the presence of POPE/POPG (*filled circles*) and POPC/SM/Chol (*open circles*). Experiments were performed at 37 °C with 15 min of incubation time prior to measurements. Curve fitting was achieved using a logistic model.

Discussion

Relationship between Live Cells and Membrane Models—The mechanism by which AMPs interact with bacteria or eukaryotic cells is largely unknown because of the cell complexity; elucidating the mode of action at molecular level is particularly difficult because of challenges in identifying interactions between peptides and complexes/domains within cells or cellular downstream effects. To examine specific molecular interactions, models are built to represent important features under investigation. Unfortunately, the correlation between live cell and membrane model experiments is too often deceptive. For instance, Mac1 inhibits *S. aureus* at a lower concentration than *E. coli* (Table 1), yet it disrupts model membranes that mimic the composition of these cells within identical potency (Table 2 and Fig. 3), and it adopts a similar amphipathic helical structure, a key event in AMPs lytic activity, in both environments (Fig. 7). Liposomes clearly are missing many important cellular features, for instance the LPS layer of the outer membrane in *E. coli* or the peptidoglycan layer in *S. aureus.* Although these layers could significantly modulate the peptide lytic activity, LPS did not prevent Mac1 adopting a helical structure (Fig. 7). Interestingly, *E. coli* depleted of O-antigen chain on LPS was more vulnerable to both peptides (Table 1), but SYTOX Green uptake was similar to the type strain *E. coli*, indicating that a thicker LPS layer did not prevent the peptides from damaging the inner membrane. Also, ζ-potential measurements suggested that Mac1 exerts its action by direct interaction with the anionic membranes rather than intracellular components, as suggested by similar membrane potential reduction obtained when Mac1 was incubated with bacteria or with model membranes (Fig. 6). Finally, Mac1 lysed both *E. coli* and *S. aureus* membranes at similar concentrations (Table 1, SYTOX Green uptake assays), and therefore, *in vitro* and *in vivo* data presented in this study trend to the same conclusion: Mac1 disrupts *E. coli* and *S. aureus* with a similar mechanism.

So why such difference in MIC? A possibility to explain these differences is the ability of bacteria to repair their damaged membranes. This proposition requires further investigation, and possibly *E. coli* (and Gram-negative in general) are more efficient than *S. aureus* (Gram-positive) in maintaining their membrane homeostasis (27), hence the differences in bacteri-

TABLE 2

Mac1 lytic activity (LC_{50}) in single and competitive lipid environments in terms of peptide per vesicles

The values are given in μM. Aliquots of peptide were added to a fixed LUV concentration of 100 μM made of equal amounts of dye-filled LUV* and dye-free LUV of similar lipid composition for single environments, whereas competitive lipid environments were made by mixing dye-filled LUV* with dye-free LUV of a different lipid composition. The LC_{50} values were obtained fitting with a logistic function; errors are standard deviations of the fit.

	POPC/SM/Chol*	POPE/POPG*	POPG/TOCL*
POPC/SM/Chol	>16	1.1 ± 0.2	2.1 ± 0.1
POPE/POPG	>16	2.8 ± 0.1	2.1 ± 0.2
POPG/TOCL	>16	13.2 ± 0.3	5.4 ± 0.2

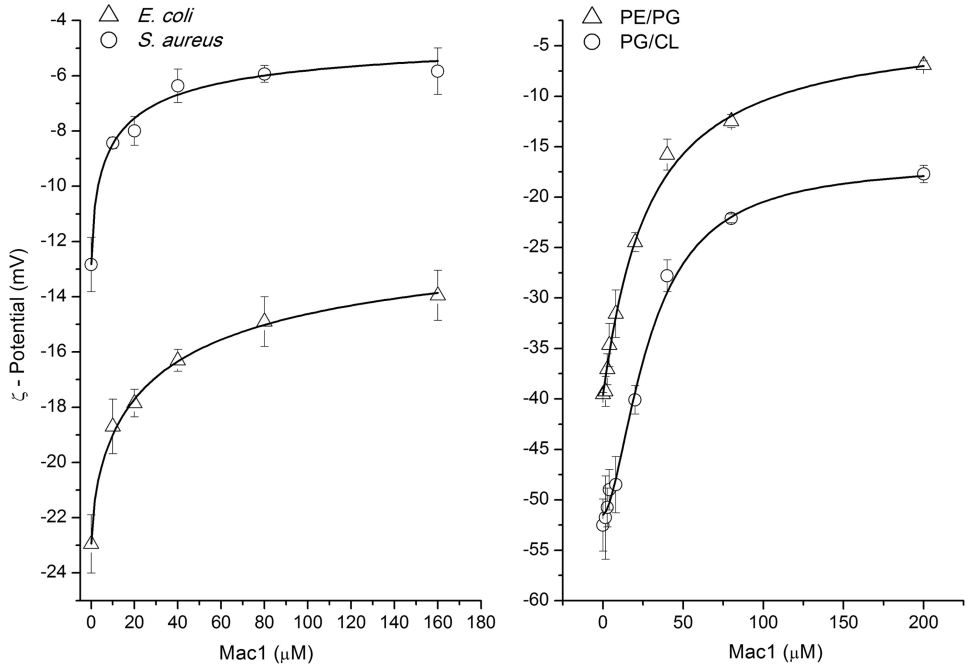

FIGURE 6. *Right panel*, ζ-potential of 200 μM POPE/POPG 7:3 (*triangles*) and POPG/TOCL 3:2 (*circles*) LUV in 50 mM NaCl buffer (phosphate pH 7) and upon titration of Mac1. *Left panel*, ζ-potential of *E. coli* (*triangles*) and *S. aureus* (*circles*) at 10^7 colony formation units in PBS. *Error bars* are standard deviations from three averaged experiments (100 runs per experiments) performed at room temperature with a 40 V potential.

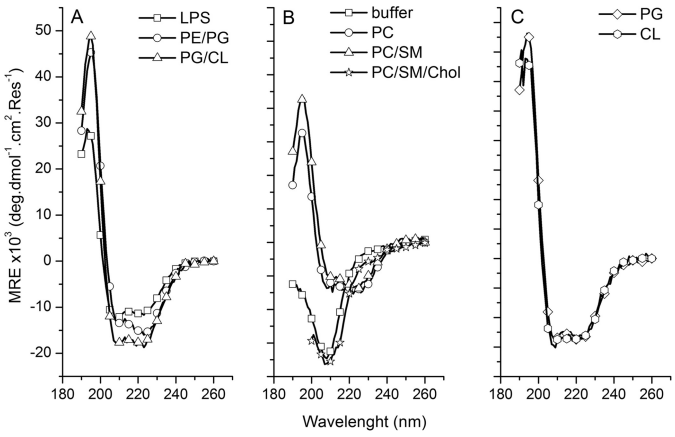

FIGURE 7. **CD spectra of Mac1 were obtained with 100 μm Mac1 in the presence of lipid vesicles at a lipid to peptide molar ratio of 50:1.** *A*, LPS micelles at 2 mg/ml (*squares*), POPE/POPG LUV (*circles*), and POPG/TOCL LUV (*triangles*). *B*, buffer (*squares*), POPC (*circles*), POPC/SM (*triangles*), and POPC/SM/Chol (*stars*). *C*, POPG (*diamonds*) and TOCL (*octagons*). The lipid background was subtracted, and three scans were accumulated at 37 °C.

cidal activities. This is supported by membrane disruption observed in bacteria (Fig. 2) occurring at lower concentrations than respective MIC (Table 1).

Electrostatic Interactions Modulate Mac1 Concentration at the Membrane but Reduce Lytic Activity—The electrostatic interactions between cationic AMP and negatively charged membrane surfaces are commonly reported to explain the specific affinity for particular bacterial strains or against eukaryotic cells (4, 28, 29). Thus, Mac1 was expected to possess a weak ability to disrupt the neutral model membranes composed of POPC/Chol/SM that mimic hRBC membranes but to strongly compromise negatively charged vesicles that mimic *S. aureus* or *E. coli* membranes. However, previous dye leakage experiments have shown that Mac1 disrupts POPC vesicles with greater efficiency than negatively charged membranes (15). This indicates that not only are electrostatic interactions important, but also the stiffness of the membrane can strongly limit peptide binding to lipid bilayers. In particular, SM and Chol that exist in high concentration in mammalian cells are known to increase lipid membrane order and to segregate and form more rigid domains (*i.e.* "raft"-like domains) in fluid cell membranes (30). Lytic activity was considerably reduced in the presence of Chol, which supports a likely role in protection of the host cell. For instance, the AMP pardaxin has reduced backbone dynamics and channel forming activity when inserted into cholesterol-rich POPC bilayers (31), and the presence of 25% Chol in POPC bilayers reduces the insertion of gramicidin S into membranes, when compared with POPC membranes (32). The selectivity of AMPs toward bacterial membrane, over mammalian cells, might be driven by the fluidity of the targeted membrane. Binding and insertion into fluid membranes, but not in more ordered membranes, is supported by the ability of Mac1 to form helical structures in the presence of POPC (13) and POPC/SM but not POPC/SM/Chol membranes (Fig. 7). A weaker binding affinity prevented the formation of an amphipathic helical structure that would allow the hydrophobic side to penetrate into the hydrophobic core of the membrane with the hydrophilic side exposed to the aqueous medium (33). A low ability to insert into liquid-ordered membranes explains the low hemolytic activity of Mac1 (Table 1). This is a hallmark of many pore-forming peptides that adopt an amphipathic structure to self-associate into the membrane and destabilize the membrane bilayer structure (2, 3, 28, 34).

Furthermore, electrostatic attractions were shown to enhance the binding affinity of Mac1 toward membranes of greater negative potential (Figs. 3–5), leading to an increase in peptide helical content (Fig. 7). No significant differences were

observed in the overall helicity of Mac1 when incubated with POPG or TOCL bilayers. Because both lipids are anionic, the structure of the anionic lipid is not a critical feature for AMP binding affinity. However, Mac1 showed a lower ability to disrupt and cause leakage of vesicles composed of 100% anionic lipids (PG/CL membranes) than vesicles made with 30% anionic lipids (PE/PG membranes). Therefore, strong electrostatic attractions between the peptide and the lipid headgroups not only increase the peptide accumulation but may lock the peptide at the membrane interface, reducing the penetration and hence the peptide lytic activity. This effect can explain the low anticancer activity of Mac1. Because cancer cells also possess greater content of anionic membrane lipids than healthy cells, the similar activity of Mac1 against HeLa and mcf-7 cells *versus* red blood cells further supports a complex relation between hydrophobicity and electrostatic interactions. Nature apparently has designed an AMP for Australian tree frogs that is specific to Gram-positive bacteria and not just cell membranes with high anionic lipid content.

Finally, the important aspect in the development of novel drugs is that AMPs confront several potential cellular targets, which could dramatically affect their potency. For instance, we have shown that although Mac1 can disrupt *E. coli*-like model membranes, when in the presence of both *E. coli*- and *S. aureus*-like membranes, the peptide has a preference for *S. aureus* model membranes (Fig. 5). Therefore, by extrapolation, we hypothesize that Mac1 could target and clear a *S. aureus* infection before killing symbiotic *E. coli* bacteria or becoming hemolytic.

Mode of Action of Mac1 against Cell Membranes—To better develop AMP as viable alternatives or complements to classic antibiotics, their mechanism of action should be determined. This is a gargantuan task because the majority of these peptides do not target a specific stereo-structure but instead adsorb onto and insert into lipid bilayers via a multistep mechanism that is likely dependent on the lipid composition of the membrane (13).

Through this study, it was shown that binding affinity toward a negatively charged membrane is not the sole parameter that modulates the ability of Mac1 to bind and disrupt lipid bilayers. In fact, a complex ratio between surface charge and membrane order is likely to promote the optimal peptide activity and thus may be responsible for the specific antibacterial concentrations. The difference in fluidity or membrane order between *E. coli* membrane and *S. aureus* membrane should be further investigated. Nevertheless, Mac1 was shown to preferentially bind *S. aureus*-like membranes, with the greater negative membrane potential, than *E. coli* membranes, and a higher membrane-bound peptide population could also be responsible for the respective bactericidal concentrations.

Finally and importantly, we indirectly demonstrated that bacteria can repair their injured membranes in nutrient-rich medium or sustain heavy membrane damage before growth inhibition occurred. Indeed, Mac1 disrupted the lipid membrane structure of *E. coli* and *S. aureus* with a similar mode of action, but inhibition occurred at much greater concentrations. Therefore, we propose that on top of the specific mode of action of AMP, bacterial membrane repair and the ability to sustain different amounts of damage may modulate the bactericidal potency.

Author Contributions—M.-A. S. conceived and coordinated the study. F. S. gave conceptual advice. M.-A. S., F. S., and S. T. H. wrote the paper. M.-A. S., S. T. H., and D. K. W. designed, performed, and analyzed the experiments. All authors reviewed the results and approved the final version of the manuscript.

References

1. Bahar, A. A., and Ren, D. (2013) Antimicrobial peptides. *Pharmaceuticals* **6,** 1543–1575
2. Yeaman, M. R., and Yount, N. Y. (2003) Mechanisms of antimicrobial peptide action and resistance. *Pharmacol. Rev.* **55,** 27–55
3. Shai, Y. (2002) Mode of action of membrane active antimicrobial peptides. *Biopolymers* **66,** 236–248
4. Epand, R. F., Savage, P. B., and Epand, R. M. (2007) Bacterial lipid composition and the antimicrobial efficacy of cationic steroid compounds (Ceragenins). *Biochim. Biophys. Acta* **1768,** 2500–2509
5. Sudheendra, U. S., Dhople, V., Datta, A., Kar, R. K., Shelburne, C. E., Bhunia, A., and Ramamoorthy, A. (2015) Membrane disruptive antimicrobial activities of human beta-defensin-3 analogs. *Eur. J. Med. Chem.* **91,** 91–99
6. Beining, P. R., Huff, E., Prescott, B., and Theodore, T. S. (1975) Characterization of the lipids of mesosomal vesicles and plasma membranes from *Staphylococcus aureus*. *J. Bacteriol.* **121,** 137–143
7. Morein, S., Andersson, A., Rilfors, L., and Lindblom, G. (1996) Wild-type *Escherichia coli* cells regulate the membrane lipid composition in a "window" between gel and non-lamellar structures. *J. Biol. Chem.* **271,** 6801–6809
8. Salvioli, G., Rioli, G., Lugli, R., and Salati, R. (1978) Membrane lipid composition of red blood cells in liver disease: regression of spur cell anaemia after infusion of polyunsaturated phosphatidylcholine. *Gut* **19,** 844–850
9. Thennarasu, S., Tan, A., Penumatchu, R., Shelburne, C. E., Heyl, D. L., and Ramamoorthy, A. (2010) Antimicrobial and membrane disrupting activities of a peptide derived from the human cathelicidin antimicrobial peptide LL37. *Biophys. J.* **98,** 248–257
10. Rozek, T., Waugh, R. J., Steinborner, S. T., Bowie, J. H., Tyler, M. J., and Wallace, J. C. (1998) The maculatin peptides from the skin glands of the tree frog *Litoria genimaculata*: a comparison of the structures and antibacterial activities of maculatin 1.1 and caerin 1.1. *J. Pept. Sci.* **4,** 111–115
11. Chia, C. S., Gong, Y., Bowie, J. H., Zuegg, J., and Cooper, M. A. (2011) Membrane binding and perturbation studies of the antimicrobial peptides caerin, citropin, and maculatin. *Biopolymers* **96,** 147–157
12. Chia, B. C., Carver, J. A., Mulhern, T. D., and Bowie, J. H. (2000) Maculatin 1.1, an anti-microbial peptide from the Australian tree frog, *Litoria genimaculata* solution structure and biological activity. *Eur. J. Biochem.* **267,** 1894–1908
13. Sani, M. A., Whitwell, T. C., and Separovic, F. (2012) Lipid composition regulates the conformation and insertion of the antimicrobial peptide maculatin 1.1. *Biochim. Biophys. Acta* **1818,** 205–211
14. Sani, M. A., Whitwell, T. C., Gehman, J. D., Robins-Browne, R. M., Pantarat, N., Attard, T. J., Reynolds, E. C., O'Brien-Simpson, N. M., and Separovic, F. (2013) Maculatin 1.1 disrupts *Staphylococcus aureus* lipid membranes via a pore mechanism. *Antimicrob. Agents Chemother.* **57,** 3593–3600
15. Sani, M. A., Gagne, E., Gehman, J. D., Whitwell, T. C., and Separovic, F. (2014) Dye-release assay for investigation of antimicrobial peptide activity in a competitive lipid environment. *Eur. Biophys. J.* **43,** 445–450
16. Sani, M. A., Dufourc, E. J., and Gröbner, G. (2009) How does the Bax-α1 targeting sequence interact with mitochondrial membranes? The role of cardiolipin. *Biochim. Biophys. Acta* **1788,** 623–631
17. Wiegand, I., Hilpert, K., and Hancock, R. E. (2008) Agar and broth dilution methods to determine the minimal inhibitory concentration (MIC) of antimicrobial substances. *Nat. Protoc.* **3,** 163–175
18. Torcato, I. M., Huang, Y. H., Franquelim, H. G., Gaspar, D., Craik, D. J.,

Castanho, M. A., and Troeira Henriques, S. (2013) Design and characterization of novel antimicrobial peptides, R-BP100 and RW-BP100, with activity against Gram-negative and Gram-positive bacteria. *Biochim. Biophys. Acta* **1828,** 944–955
19. Roth, B. L., Poot, M., Yue, S. T., and Millard, P. J. (1997) Bacterial viability and antibiotic susceptibility testing with SYTOX green nucleic acid stain. *Appl. Environ. Microbiol.* **63,** 2421–2431
20. Shepherd, N. E., Hoang, H. N., Abbenante, G., and Fairlie, D. P. (2005) Single turn peptide α helices with exceptional stability in water. *J. Am. Chem. Soc.* **127,** 2974–2983
21. Henriques, S. T., Pattenden, L. K., Aguilar, M. I., and Castanho, M. A. (2008) PrP(106–126) does not interact with membranes under physiological conditions. *Biophys. J.* **95,** 1877–1889
22. Henriques, S. T., Huang, Y. H., Rosengren, K. J., Franquelim, H. G., Carvalho, F. A., Johnson, A., Sonza, S., Tachedjian, G., Castanho, M. A., Daly, N. L., and Craik, D. J. (2011) Decoding the membrane activity of the cyclotide kalata B1: the importance of phosphatidylethanolamine phospholipids and lipid organization on hemolytic and anti-HIV activities. *J. Biol. Chem.* **286,** 24231–24241
23. Sando, L., Henriques, S. T., Foley, F., Simonsen, S. M., Daly, N. L., Hall, K. N., Gustafson, K. R., Aguilar, M. I., and Craik, D. J. (2011) A Synthetic mirror image of kalata B1 reveals that cyclotide activity is independent of a protein receptor. *Chembiochem* **12,** 2456–2462
24. Gehman, J. D., Luc, F., Hall, K., Lee, T. H., Boland, M. P., Pukala, T. L., Bowie, J. H., Aguilar, M. I., and Separovic, F. (2008) Effect of antimicrobial peptides from Australian tree frogs on anionic phospholipid membranes. *Biochemistry* **47,** 8557–8565
25. Jamasbi, E., Batinovic, S., Sharples, R. A., Sani, M. A., Robins-Browne, R. M., Wade, J. D., Separovic, F., and Hossain, M. A. (2014) Melittin peptides exhibit different activity on different cells and model membranes. *Amino Acids* **46,** 2759–2766
26. Hoskin, D. W., and Ramamoorthy, A. (2008) Studies on anticancer activities of antimicrobial peptides. *Biochim. Biophys. Acta* **1778,** 357–375
27. Hurst, A. (1977) Bacterial injury. *Can. J. Microbiol.* **23,** 935–944
28. Brogden, K. A. (2005) Antimicrobial peptides: pore formers or metabolic inhibitors in bacteria? *Nat. Rev. Microbiol.* **3,** 238–250
29. Zasloff, M. (2002) Antimicrobial peptides of multicellular organisms. *Nature* **415,** 389–395
30. Filippov, A., Orädd, G., and Lindblom, G. (2004) Lipid lateral diffusion in ordered and disordered phases in raft mixtures. *Biophys. J.* **86,** 891–896
31. Ramamoorthy, A., Lee, D. K., Narasimhaswamy, T., and Nanga, R. P. (2010) Cholesterol reduces pardaxin's dynamics-a barrel-stave mechanism of membrane disruption investigated by solid-state NMR. *Biochim. Biophys. Acta* **1798,** 223–227
32. Prenner, E. J., Lewis, R. N., Jelokhani-Niaraki, M., Hodges, R. S., and McElhaney, R. N. (2001) Cholesterol attenuates the interaction of the antimicrobial peptide gramicidin S with phospholipid bilayer membranes. *Biochim. Biophys. Acta* **1510,** 83–92
33. Tossi, A., Sandri, L., and Giangaspero, A. (2000) Amphipathic, α-helical antimicrobial peptides. *Biopolymers* **55,** 4–30
34. Shai, Y. (1999) Mechanism of the binding, insertion and destabilization of phospholipid bilayer membranes by α-helical antimicrobial and cell nonselective membrane-lytic peptides. *Biochim. Biophys. Acta* **1462,** 55–70

Bacteria May Cope Differently from Similar Membrane Damage Caused by the Australian Tree Frog Antimicrobial Peptide Maculatin 1.1

Marc-Antoine Sani, Sónia Troeira Henriques, Daniel Weber and Frances Separovic

J. Biol. Chem. 2015, 290:19853-19862.
doi: 10.1074/jbc.M115.643262 originally published online June 22, 2015